present, we cannot give a completely adequate explanation for its presence. There is no other evidence of extremely high densities in the coma. But there are other possible explanations for the emission. For example, following the suggestion of Gladstone (*10*), it is possible that intense electric fields in the coma could change the 1128/8446 branching ratio so that the 1128 Å transition is no longer forbidden. Other possible explanations may exist. However, we want to emphasize that the detection is real, and not due to instrumental effects.

Other astrophysical objects seem to indicate that similar processes are occurring. Thus we may find in the future that the 1128 Å line will become a standard diagnostic for many classes of objects. For example, quasar emission-line clouds have been shown to be optically thick in 8446 Å, an optical line that populates the $3p\ ^3P$ state of OI, the originating state for 1128 Å emission (*11*). M-giant chromospheres have exhibited 1641 Å emission, another forbidden transition resulting from a cascade through the $3p\ ^3P$ state (*12*). Unfortunately, observations of these dim targets at 1128 Å will probably have to wait until the FUSE experiment flies.

REFERENCES AND NOTES

1. W. Cash *et al.*, *Exper. Astron.* **1**, 123 (1989).
2. T. A. Cook, W. Cash, J. C. Green, in preparation.
3. I. S. Bowen, *Pub. A.S.P.* **59**, 196 (1947).
4. P. D. Feldman *et al.*, *NASA Special Publication SP-393* (NASA, Washington, DC, 1974), p. 773.
5. S. A. Stern, thesis, University of Colorado (1989).
6. S. Bashkin and J. Stoner, *Atomic Energy Levels and Grotrian Diagrams* (North-Holland, Amsterdam, 1975), vol. 1.
7. There is an allowed transition from the $7d\ ^3P$ state of CI within the allowed error in the wavelength identification, however, it is unlikely that this could be the source of the emission, given the lack of accompanying lines out of the $8d\ ^3P$ or $6d\ ^3P$ states.
8. M. C. Festou and P. D. Feldman, *Astron. Astrophys.* **103**, 154 (1981).
9. P. Swings, *Annal. Astrophys.* **25, 165 (1962).**
10. R. Gladstone, private communication.
11. S. Grandi, *Astrophys. J.* **268**, 591 (1983).
12. A. Brown, M. Ferraz, C. Jordan, *The Universe at Ultraviolet Wavelengths: The First Two Years of IUE*, R. D. Chapman, Ed. (NASA CP-2171), (NASA, Washington, DC, 1981), p. 297.

13. The authors thank J. Van Overeem of the NASA/Wallops Island Flight Facility for his invaluable assistance in making this observation possible. We would also like to thank P. Feldman, M. Shull, T. Snow, and J. Stocke for useful scientific discussions and D. Yeomans for providing accurate and up-to-date orbital elements for comet Austin. This work was supported under NASA grant NSG 5303.

25 May 1990; accepted 20 November 1990

Phase Transition and Thermal Expansion of $MgSiO_3$ Perovskite

YANBIN WANG, DONALD J. WEIDNER, ROBERT C. LIEBERMANN, XING LIU, JAIDONG KO, MICHAEL T. VAUGHAN, YUSHENG ZHAO, AMIR YEGANEH-HAERI, ROSEMARY E. G. PACALO

Results from in situ x-ray diffraction experiments with a DIA-type cubic anvil apparatus (SAM 85) reveal that $MgSiO_3$ perovskite transforms from the orthorhombic *Pbnm* symmetry to another perovskite-type structure above 600 kelvin (K) at pressures of 7.3 gigapascals; the apparent volume increase across the transition is 0.7%. Unit-cell volume increased linearly with temperature, both below (1.44×10^{-5} K^{-1}) and above (1.55×10^{-5} K^{-1}) the transition. These results indicate that the physical properties measured on the *Pbnm* phase should be used with great caution because they may not be applicable to the earth's lower mantle. A density analysis based on the new data yields an iron content of 10.4 weight percent for a pyrolite composition under conditions corresponding to the lower mantle. All current equation-of-state data are compatible with constant chemical composition in the upper and lower mantle; thus, these data imply that a chemically layered mantle is unnecessary, and whole-mantle convection is possible.

AT PRESSURES GREATER THAN 23 GPa, all of the major minerals of the earth's upper mantle transform under high temperatures to phase assemblages dominated by $(Mg,Fe)SiO_3$ perovskite (*1*). Therefore, the properties of this silicate perovskite control those of the earth's lower mantle (depths of 650 to 2900 km) and knowledge of its crystal structure and response to changes in temperature and pressure are crucial in understanding physical and chemical processes of the mantle. Under ambient conditions, the crystal structure of the metastable perovskite is orthorhombic, with space group *Pbnm* (*2*), which has been assumed to be the stable structure throughout the lower mantle. However, many perovskite-structure materials with ABO_3 composition undergo sequences of phase transitions with increasing pressure and temperature, and these transitions are associated with dramatic changes in physical properties (*3*). Earlier conclusions that the *Pbnm* distortion remains unchanged with increasing temperature and pressure (*4, 5*) have been shown to be incorrect (*6–9*). Transmission electron microscopy studies on twin-domain structures in $MgSiO_3$ perovskite quenched from 26 GPa and 1873 K provide indirect evidence of the presence of structural phase transitions (*10*). At atmospheric pressure thermal expansion measurements have been limited to a few hundred kelvin, above which the perovskite structure becomes unstable (*4, 6, 9*). Recently, Mao *et al.* (*11*) carried out a simultaneous high-pressure and high-temperature study using an externally heated diamond-anvil cell; however, as the temperature was increased from 300 to 877 K, the pressure decreased from 27 to 4 GPa.

By using a large-volume, high-pressure apparatus in conjunction with a synchrotron x-ray source, we have been able to stabilize $MgSiO_3$ perovskite to temperatures up to 1253 K at constant pressure and to study the evolution of its crystal structure by x-ray diffraction. The experiment was performed in a DIA-6–type cubic-anvil apparatus (SAM-85) at the superconducting wiggler

Mineral Physics Institute and Department of Earth and Space Sciences, State University of New York at Stony Brook, Stony Brook, NY 11794.

Table 1. Zero-pressure linear compressibilities of $(Mg,Fe)SiO_3$ perovskite at 300 K. P_{max}, maximum pressure in the measurements; pressure medium: M-E, methanol-ethanol; M-E-W, methanol-ethanol-water; Ne, neon; sample form: SC, single crystal; P, powder. References (*7*), (*8*), and (*11*) give angle-dispersive x-ray data from the diamond cell; (*16*) gives Brillouin spectroscopy data at 1 bar.

β_a (TPa^{-1})	β_b (TPa^{-1})	β_c (TPa^{-1})	P_{max} (GPa)	x	Pressure medium	Sample	References
1.31	1.20	1.56	0	0	—	SC	(*16*)
1.41	1.07	1.57	10	0	M-E-W	SC	(*8*)
1.30	1.04	1.24	13	0	M-E, Ne	SC	(*7*)
1.29	1.05	1.33	30	0 to 0.2	Ne	P	(*11*)
1.29	1.03	1.31	7.3	0	NaCl	P	This study

beam line (X-17) of the National Synchrotron Light Source (*12*). The perovskite specimen was synthesized in a 2000-ton uniaxial split-sphere apparatus (USSA-2000) at 26 GPa and 2273 K (*10*). A pellet of the polycrystalline sample, 1 mm in diameter and 0.4 mm in length, was placed in a cell assembly described in (*13*). To reduce nonhydrostatic stress in the assembly, we embedded the specimen in NaCl, which also served as a pressure calibrant (*14*). During the experiment, we first applied pressure at 300 K, and then elevated temperature under constant load; no drop in pressure was observed during heating. Energy-dispersive x-ray diffraction spectra were collected at a 2θ of 7.5° with a Ge(Li) detector and a multichannel analyzer. The diffraction geometry provided sufficient resolution to quantify the *Pbnm* distortion of the silicate perovskite; in most cases, at least eight distinct peaks, 111, 020, 112, 200, 113, 040, 224, and 400, were used to refine the cell parameters at a given pressure-temperature condition (*15*). At 300 K, the *Pbnm* distortion increased with pressure to 7.3 GPa, in a manner similar to that shown by single crystal (*7, 8*) and synchrotron powder x-ray (*11*) data obtained with the diamond cell and under hydrostatic pressure (Table 1). The general trend of the cell-edge compressibilities (β) $\beta_c \geq \beta_a > \beta_b$ is consistent in most of these studies. The pressure scale that we used may be somewhat different from those in the diamond cell studies because of different pressure distribution and diffraction geometry; however, the agreement suggests that the effects of deviatoric stress in our experiment were insignificant (*17*).

At 7.3 GPa, we observed a structural phase transition in $MgSiO_3$ perovskite near 600 K and measured the isobaric thermal expansion up to 1253 K. As the specimen was heated, most of the observed *d*-spacings changed systematically with temperature to 573 K. In contrast, the *d*-spacings increased sharply between 573 and 623 K. The *d*-spacings for the doublets 110/002 and 220/004 decreased slightly from 400 to 573 K and then shifted abruptly to higher values at 623 K in association with a dramatic decrease in peak intensity. A particularly interesting example is the change in spacing of a minor reflection with an observed *d*-spacing (d_{obs}) of 1.5 Å (Fig. 1). Below 573 K, the reflection can be satisfactorily assigned to the *Pbnm* planes 131 and 310 (d_{131} and d_{310} in Fig. 1). Above 623 K, however, when an attempt is made to refine the cell parameters in the *Pbnm* space group, all of the calculated d_{131} and d_{310} systematically deviate from the observed values; the discrepancy is three to five times the estimated error. This disagreement clearly indicates that the high-temperature phase is incompatible with the space group *Pbnm*.

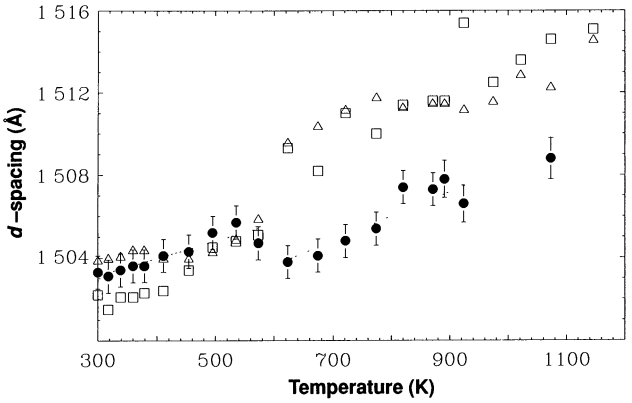

Fig. 1. Variation of a minor reflection d_{obs} (solid circles) observed in $MgSiO_3$ perovskite as a function of temperature at 7.3 GPa. Squares and triangles are, respectively, calculated d_{131} and d_{310} for the refined *Pbnm* cell parameters in Fig. 2. Below 573 K, the observed and calculated *d*-spacings are in good agreement. The discrepancy between d_{obs} and $d_{131}(d_{310})$ above 623 K indicates that the *Pbnm* space group is incompatible with the crystal structure and that a structural phase transition has occurred near 600 K. Vertical bars are estimated standard errors in measuring d_{obs} (*15*).

The above observations indicate that a structural phase transition occurs in $MgSiO_3$ perovskite near 600 K at 7.3 GPa. Despite this transition, the diffraction spectra can still be indexed on the basis of the *Pbnm* space group if reflections such as those from the 131 and 310 planes discussed above are excluded. We indexed the spectra from 300 to 1146 K in this manner; the resultant orthorhombic cell parameters *a*, *b*, and *c* all increase abruptly between 573 and 623 K, and the corresponding unit-cell volume increases by about 0.7% in this temperature interval (Fig. 2). Both below and above 623 K, the cell volume increased linearly with temperature, with volumetric thermal expansivities (α_v) of 1.44×10^{-5} and 1.55×10^{-5} K^{-1}, respectively (*18*). At 7.3 GPa, the perovskite-type structure was retained up to 1253 K, above which the sample became amorphous and then rapidly recrystallized into the low-pressure enstatite phase. The temperature range of the volume determinations used to calculate α_v is about 400 K greater than in earlier studies.

Our low-temperature data (<573 K) obtained at elevated pressure are in excellent agreement with the single-crystal x-ray diffraction data for $MgSiO_3$ (*6*) and synchrotron x-ray powder-diffraction data for $Mg_{0.9}Fe_{0.1}SiO_3$ (*9*) obtained at atmospheric pressure (Fig. 3). A more interesting comparison is with the data for $Mg_{0.9}Fe_{0.1}SiO_3$ perovskite obtained by Mao *et al.* (*11*) at

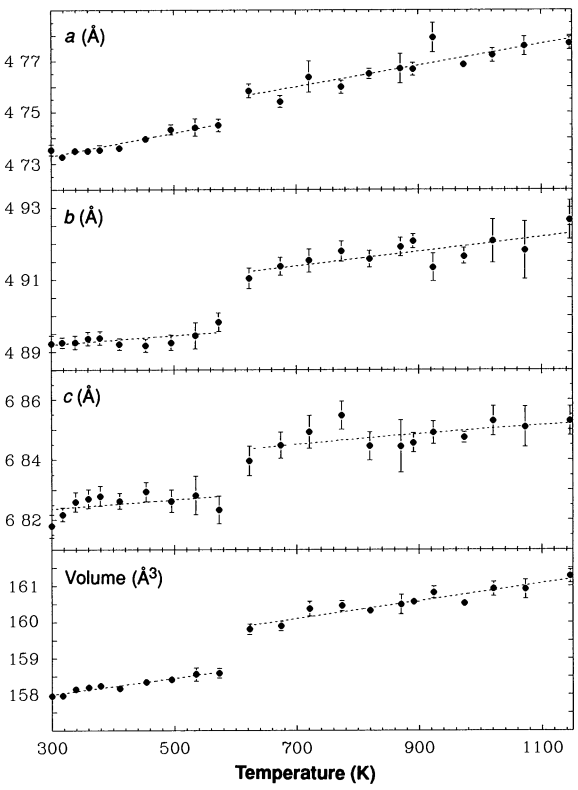

Fig. 2. Unit-cell parameters, from top to bottom, *a*, *b*, *c*, and *V* of $MgSiO_3$ perovskite as a function of temperature. The discontinuity in all the parameters between 573 and 623 K indicates a phase transition. Error bars represent 1 SD.

high pressures. Assuming that the effects of pressure and temperature can be treated individually, we have corrected their data to 7.3 GPa using their room-temperature equation of state. These data agree remarkably well with ours (Fig. 3) and exhibit a similar volume increase between 573 and 623 K. This comparison demonstrates that the behavior we observed in $MgSiO_3$ perovskite is also exhibited by iron-containing perovskite at higher pressures.

Knittle *et al.* (*4*) obtained unit-cell volumes of a $Mg_{0.88}Fe_{0.12}SiO_3$ perovskite at 1 bar to 840 K (Fig. 3). Their volume versus temperature data exhibit a significant concave-upward curvature above 500 K, which was interpreted as indicating an increase of α_v to an average value of 4×10^{-5} K^{-1} between 450 and 840 K. The concave curvature of their data falls in the temperature range near the phase transition observed in our experiments. In consideration of the large uncertainties in both their volume and temperature measurements, the agreement with our data is good up to 840 K, above which their sample reverted to the low-pressure enstatite phase. Our data above 850 K strongly indicate that the concave behavior between 600 and 840 K does not represent high-temperature thermal expansion of the silicate perovskite; instead, the agreement of their observed volume change with ours leads us to conclude that their data above 550 K also reflects the presence of a phase transition.

Inasmuch as the high-temperature (high-entropy) phase is the larger volume phase, the Capeyron slope must be positive. However, within the resolution of all of the available data, no increase in transition temperature with pressure is required. We interpret these varied data to indicate that the phase transition is independent of iron content as well as whether the starting sample was synthesized in a laser-heated diamond-anvil cell at relatively high pressures and temperatures (*4, 11*) or in a large-volume press at correspondingly lower pressures and temperatures [(*6, 9*); this study]. Furthermore, Knittle *et al.*'s observation that the volume increase was reversible on cooling from 820 K [see figure 1 of (*4*)] implies that the phase transition causing this volume increase is reversible (Fig. 3) on the time scale of the laboratory experiment.

The chemical composition of the earth's lower mantle can be constrained by comparing the seismically derived density with that calculated from an equation of state. This comparison primarily bounds the iron content of the lower mantle. The accuracy of the conclusion is mostly limited by the uncertainty in the thermal expansion coefficient of the constitutive material (*4, 19, 20, 21*) (Fig. 4), whereas uncertainties in the zero-pressure bulk modulus (K_0) of the perovskite phase and its pressure derivative $[(dK/dP)_0]$, as well as the silica content (indicated by the Mg/Si ratio), do not have a large effect on the deduced iron content (variations shown in Fig. 4 are for a reference point in the lower mantle arbitrarily chosen as a depth of 1071 km). Our preferred model of these parameters (given by the arrowheads in Fig. 4 including $\alpha_v = 1.5 \times 10^{-5}$ K^{-1} for the high-temperature phase from this study) corresponds to an iron content of 10.4% for a pyrolite stoichiometry (*22*). This iron content is consistent with that deduced for the upper mantle; thus, a chemically layered model is rendered unnecessary.

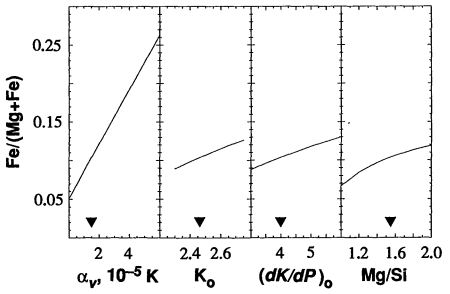

Fig. 4. The dependence of the iron content of the earth's lower mantle at 1071 km depth on model parameters including thermal expansion (α_v), bulk modulus (K_0) and its pressure derivative $[(dK/dP)_0]$, and the ratio of divalent to tetravalent cations (Mg/Si), which ranges from 1.0 (pyroxene stoichiometry) to 2.0 (olivine). The density at this depth is 4.621 g cm^{-3}, and pressure is 41.86 GPa [from the PREM model (*24*)]. The temperature at this depth is set at 2004 K (*25*). Arrowheads indicate our preferred model values. The high-temperature phase is assumed to be stable at 1071 km with a room-temperature molar volume of 24.725 cm^3 $[=V_0^{Pbnm}(1 + 0.7\%)]$; $K_0 = 246.5$ GPa (*16*); $(dK/dP)_0 = 4$. With these parameters we infer an iron-content of 10.4% at 1071 km by matching the seismic density.

The conclusion of Jeanloz and Knittle [(*19*); see also (*4*)] that the lower mantle must have a greater iron content than the upper mantle rests mainly on their preferred value of $\alpha_v = 4 \times 10^{-5}$ K^{-1} for the high-temperature thermal expansivity of silicate perovskite. However, several studies have shown that the upper mantle composition would be compatible with the seismic properties of the lower mantle if $\alpha_v \leq 2.5 \times 10^{-5}$ K^{-1} for the perovskite phase (*20, 21, 23*). We have demonstrated that the results of the experiments on which the high values of thermal expansion are based are probably misleading because of the presence of a phase transition (*4, 11*).

Thermal expansion will generally decrease with pressure and increase with temperature (*23*); both effects have been ignored in our calculations. Furthermore, Wang *et al.* (*10*) provided evidence that $MgSiO_3$ perovskite may undergo additional phase transitions to tetragonal or cubic symmetry under mantle conditions. Such changes may yield an effective thermal expansion that is much different than those we have determined. Knowledge of the composition of the lower mantle must still await definitive experiments that monitor volume under the pressure and temperature conditions of the lower mantle. Nonetheless, all current data that pertain to the equation of state can be rationalized with no change in chemical composition between the upper and the lower mantle. Thus, on the basis of density considerations, we find no evidence of a chemical barrier to convection across the upper to lower mantle boundary.

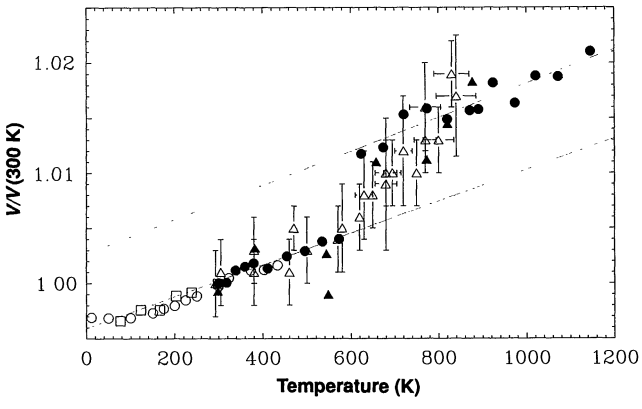

Fig. 3. Comparison of the present volumetric thermal expansion with earlier measurements on $Mg_{1-x}Fe_xSiO_3$ perovskite. All of the available data indicate that an abrupt increase in volume occurs near 600 K, consistent with the phase transition observed in this study. For clarity, only data from (*4*) ($x = 0.12$, open triangles) are shown with errors; errors reported in (*6*) ($x = 0$, open squares) and in (*9*) ($x = 0.1$, open circles) are about the size of the symbols. Data of (*11*) ($x = 0.1$, solid triangles) are corrected to a constant pressure (7.3 GPa) to be compatible with the other studies; data below 550 K were obtained at $P > 21$ GPa, those above 650 K at $P < 15$ GPa. Dotted lines are the best fit of our data (solid circles) below and above 600 K.

REFERENCES AND NOTES

1. L. G. Liu, *Geophys. Res. Lett.* **2**, 417 (1975); E. Ito, *ibid.* **4**, 72 (1977); _____, E. Takahashi, Y. Mastui, *Earth Planet. Sci. Lett.* **67**, 238 (1984).
2. E. Ito and Y. Matsui, *Earth Planet. Sci. Lett.* **38**, 443 (1978); H. Horiuchi, E. Ito, D. J. Weidner, *Am. Mineral.* **72**, 357 (1987).
3. J. B. Goodenough and J. M. Longo, in *Landolt-Bornstein, Zahlenwerte und Funktionen aus Naturwissenschaften und Technik, Neue Serie, Group III*, Band

4, Teil a (Springer-Verlag, Berlin, 1970), pp. 126–314; A. M. Glazer, *Acta Crystallogr. Sect. B* **28**, 3384 (1972); K. S. Aleksandrov, *Ferroelectrics* **14**, 801 (1976).
4. E. Knittle *et al.*, *Nature* **319**, 214 (1986).
5. E. Knittle and R. Jeanloz, *Science* **235**, 669 (1987).
6. N. L. Ross and R. M. Hazen, *Phys. Chem. Minerals* **16**, 415 (1989).
7. ———, *ibid.* **17**, 228 (1990).
8. Y. Kudoh, E. Ito, H. Takeda, *ibid.* **14**, 350 (1987).
9. J. B. Parise *et al.*, *Geophys. Res. Lett.* **17**, 2089 (1990).
10. Y. Wang *et al.*, *Science* **248**, 468 (1990).
11. H. K. Mao *et al.*, in *Annual Report of the Director* (Geophysical Laboratory, Carnegie Institution of Washington, Washington, DC, 1988–1989), p. 82.
12. High-energy white x-radiation (200 mA and 2500 MeV) was provided by a 4-tesla superconducting wiggler magnet. The incident x-ray was well collimated and the beam dimensions were 150 by 250 μm; a 400-μm-thick aluminum foil was used to filter low-energy x-rays (<20 keV), which may be harmful to the metastable perovskite. Energy-dispersive x-ray diffraction patterns were collected up to 100 keV for 300 s.
13. D. J. Weidner *et al.*, *Eos* **71**, 1620 (1990).
14. D. L. Decker, *J. Appl. Phys.* **42**, 3239 (1971).
15. The channel numbers of the multichannel analyzer were calibrated using *d* spacings of Si (NBS, SRM640a, 1982), NaCl (JCPDS No. 5-628) and $MgSiO_3$ perovskite (*2*). The calibration gives an estimated standard error 0.0008 Å. Each pressure was determined from reflections of NaCl on top of the sample, and as the sample was heated, the cell parameter of NaCl increased smoothly with temperature, in contrast to the behavior observed in the silicate perovskite (Fig. 2). On the basis of Decker's high-temperature equation of state for NaCl (*14*), the estimated pressure variation was within 0.2 GPa throughout the temperature range in the experiment.
16. A. Yeganeh-Haeri *et al.*, *Science* **243**, 787 (1989).
17. An analysis on the NaCl data indicates that the stress field in the cell assembly is approximately cylindrically symmetric, with the maximum (minimum) compressional principal stress σ_1 (σ_3) roughly parallel (perpendicular) to the cylindrical axis of the specimen. True pressure is defined by $(\sigma_1 + 2\sigma_3)/3$. At room temperature, deviatoric stress $(\sigma_1 - \sigma_3)$ increases to a maximum value of 0.3 GPa at a pressure of about 2 GPa, and then remains virtually constant at higher pressures. Thus, the value of 0.3 GPa represents the boundary condition of $(\sigma_1 - \sigma_3)$ on the cylindrical perovskite specimen, which is embedded in NaCl. The deviatoric stress decreases smoothly with temperature and is less than 0.05 GPa near 700 K (*13*).
18. Because the unit cell parameters were refined in the *Pbnm* space group, some uncertainties may have been introduced in the unit-cell volume of the high-temperature phase. However, because most of the major reflections exhibit a sharp increase in the corresponding *d*-spacings across 623 K, the apparent unit-cell volume represents a reasonable approximation to the real cell, with a multiplication factor because of change in number of formula units per cell. This approximation was further checked in an analysis where both phases were refined in pseudocubic cells. Although the estimated errors were a factor of 2 to 5 larger, a similar volume increase was observed. Volumetric thermal expansivities (that is, the slope of the data) were also similar to those shown in Fig. 1.
19. R. Jeanloz and E. Knittle, *Philos. Trans. R. Soc. London Ser. A* **328**, 377 (1989).
20. ———, in *Chemistry and Physics of Terrestrial Planets*, S. K. Saxena, Ed. (Springer-Verlag, New York, 1986), vol. 6, pp. 275–309.
21. I. Jackson, *Earth Planet Sci. Lett.* **62**, 91 (1983); M. S. T. Bukowinski and G. H. Wolf, *J. Geophys. Res.* **95**, 12583 (1989).
22. A. E. Ringwood, *Composition and Petrology of the Earth's Mantle* (McGraw-Hill, New York, 1975).
23. G. H. Wolf and M. S. T. Bukowinski, in *High Pressure Research in Mineral Physics*, M. H. Manghnani and Y. Syono, Eds. (American Geophysical Union, Washington, DC, 1987), pp. 313–331; A. Chopelas and R. Boehler, *Geophys. Res. Lett.* **16**, 1347 (1989).
24. A. M. Dziewonski and D. L. Anderson, *Phys. Earth Planet. Inter.* **25**, 297 (1981).
25. J. M. Brown and T. J. Shankland, *Geophys. J. R. Astronom. Soc.* **66**, 579 (1981).
26. We thank K. Baldwin, P. Hoversen, and W. Huebsch for technical assistance and J. B. Parise T. Gasparik, K. Leinenweber, and H. K. Mao for discussions and advice. We also thank D. Chapman, N. Lazarz, and W. Thomlinson for support from NSLS for the X17 beam line. The High Pressure Laboratory is supported by the National Science Foundation (NSF) grants EAR 89-17563 and the State University of New York at Stony Brook. This research was also supported by NSF grants EAR 88-17097, 88-04087, and 89-17119. MPI contribution No. 31.

16 October 1990; accepted 11 December 1990

Field-Based Evidence for Devolatilization in Subduction Zones: Implications for Arc Magmatism

GRAY E. BEBOUT

Metamorphic rocks on Santa Catalina Island, California, afford examination of fluid-related processes at depths of 15 to 45 kilometers in an Early Cretaceous subduction zone. A combination of field, stable isotope, and volatile content data for the Catalina Schist indicates kilometer-scale transport of large amounts of water-rich fluid with uniform oxygen and hydrogen isotope compositions. The fluids were liberated in devolatilizing, relatively low-temperature (400° to 600°C) parts of the subduction zone, primarily by chlorite-breakdown reactions. An evaluation of pertinent phase equilibria indicates that chlorite in mafic and sedimentary rocks and melange may stabilize a large volatile component to great depths (perhaps >100 kilometers), depending on the thermal structure of the subduction zone. This evidence for deep volatile subduction and large-scale flow of slab-derived, water-rich fluids lends credence to models that invoke fluid addition to sites of arc magma genesis.

SUBDUCTION TRANSFERS VOLATILE-rich, hydrothermally altered igneous rocks produced at mid-ocean ridges and sediments deposited on the sea-floor abyssal plain and in trenches to the upper mantle. At deep levels in subduction zones (>15 km), volatiles released by metamorphic devolatilization reactions play key roles in the geochemical evolution of the slab-mantle interface and in the overlying mantle wedge. Petrologic relations and trace element and isotopic systematics in arc volcanic rocks suggest that water-rich fluids flux partial melting in the source regions of arc magmatism [depths of 80 to 150 km (*1*)] and contribute slab-derived chemical components to such regions [radiogenic isotopic signatures of Pb, Sr, and Be, and trace elements (*2*)].

Direct field-based studies of the effects of fluid production and transport at depths >15 km have been lacking. Evaluations of the significance of fluid processes at great depths in subduction zones have been limited to the study of indirect products of subduction (arc volcanic rocks) and to theoretical models of thermal evolution and devolatilization (*3, 4*). Exposures of blueschists, eclogites, and other associated metamorphic rocks record relatively high-pressure, low-temperature conditions present in subduction zones at depths of 15 to 90 km (*4, 5*). They generally contain abundant veins and other evidence for fluid mobility and metasomatic interactions during metamorphism. These terranes allow direct assessments of volatile reservoirs in subducted rocks, of progressive volatile release during metamorphism, and of fluid transport mechanisms during subduction. In this report, I present stable isotope and field evidence, from blueschist and higher grade metamorphic rocks of the Catalina Schist (Santa Catalina Island, southern California). These data record the effects of progressive devolatilization and large-scale fluid transport at depths of 15 to 45 km in an Early Cretaceous subduction zone and, together with considerations of plausible subducted volatile reservoirs and rock pressure-temperature (*P-T*) histories, allow inference of the devolatilization history in deeper parts of subduction zones and its relevance to arc magmatism.

The Catalina Schist consists of three major metamorphic-tectonic units juxtaposed along low-angle faults (*6*). The structurally lowest, lawsonite-albite to blueschist facies unit is composed primarily of metasedimentary rocks, with lesser amounts of metamorphosed mafic and ultramafic rocks. This unit is structurally overlain by a unit that ranges in grade from glaucophanic greenschist to epidote amphibolite and consists primarily of metamorphosed mafic and sedimentary rocks. The structurally highest unit is amphibolite grade and contains metamafic and

Geophysical Laboratory, Carnegie Institution of Washington, 5251 Broad Branch Road, NW, Washington, DC 20015.